# In Situ Study of Polymer Brushes as Selective Barriers to Diffusion

**Hyun-Su Lee and Lynn S. Penn***

*Department of Chemistry, Drexel University, 3141 Chestnut Street, Philadelphia, Pennsylvania 19104*

*Received April 25, 2008; Revised Manuscript Received July 24, 2008*

ABSTRACT: Using the quartz crystal microbalance, we studied the formation of polymer brushes and the penetration of these brushes by chemically identical free chains. The systems studied were composed of thiol-end-functionalized polystyrene chains, toluene, and gold. Brushes were exposed to dilute solutions of free chains of molecular weight both greater than and less than that of the chains of the brush. Only the free chains of lower molecular weight penetrated the brush. These chains diffused all the way to the underlying gold surface and became grafted, while chains of larger molecular weight did not penetrate the brush to any extent whatsoever.

## I. Introduction

Polymer brushes, first noticed for their ability to stabilize suspensions of particles[1] and later for their ability to provide switchable surfaces,[2] are more recently of interest for their potential applications as diffusion barriers and molecular gates. Full exploitation of the barrier and gate behavior of polymer brushes requires a fundamental understanding of how and why certain free polymers in solution penetrate the brush and others do not. Development of such an understanding is the long-term goal of our research program on polymer brushes.

Our initial investigations of the penetration of polymer brushes by free chains were performed on systems composed of polystyrene brushes, toluene solvent, and—as the grafting surface—epoxide-derivatized silicate glass.[3,4] The brushes were formed by means of the grafting-to approach. A screening study that was part of that work indicated that only free polystyrene chains of *lower* molecular weight than the chains in the brush could penetrate it to reach the grafting surface.[3] Up to now, results in our laboratory have been obtained by means of a solution depletion method in which the concentration of free chains in solution was quantitatively analyzed versus time. This method of analysis was not only ex situ, because aliquots were removed from the reacting system for analysis, but also indirect, because the number of chains grafted to the surface was derived from the number that disappeared from solution.

The investigation described in the present paper was performed on systems composed of polystyrene brushes, toluene solvent, and—as the grafting surface—gold. These brushes, also, were formed by means of the grafting-to approach. The hypothesis made for the polystyrene brushes grafted to gold was that they would present a selective barrier to penetration by free chains and that the selectivity would be qualitatively the same as that observed previously for polymer brushes grafted to epoxide-derivatized silicate glass. This hypothesis arises from numerous theoretical discussions[5−13] indicating that the penetration of the brush by free chains is governed only by physical aspects of the brush and free chains and not by the nature of the grafting surface.

To study the polystyrene/toluene/gold system, we used a quartz crystal microbalance (QCM), which is a sensitive and practical tool for measurement of mass deposited on a solid surface from gas or liquid phase.[14−19] This method of analysis is not only in situ, because measurements are made continuously within the reacting system, but also direct, because the mass added to the grafting surface itself is sensed. Because of these capabilities, the QCM technique reveals aspects of polymer brush behavior that cannot be accessed by ex situ means. The present paper describes the use of this method to explore directly the behavior of brushes as selective barriers to penetration.

Before the experimental details and results of our study on the polystyrene/toluene/gold system are provided, a brief explanation of the QCM technique and its application to polymer brushes is presented. The QCM technique is based on the change in resonant frequency of a vibrating disk of α-quartz, a piezoelectric material, when mass is added to it.[14,15] The QCM instrument reports changes in the frequency of the fundamental vibrational mode and selected overtones as well as changes in the dissipation of vibrational energy. The Sauerbrey equation[14−19] relates the change in vibrational frequency to the change in mass of the quartz crystal,

$$\Delta m = -C\frac{\Delta f_n}{n}$$

where $\Delta m$ is the change in mass, $C$ is the mass sensitivity constant ($C = 17.7$ ng·cm$^{-2}$·Hz$^{-1}$ for an AT-cut, 5 MHz crystal), and $\Delta f_n$ is the change in frequency of the $n$th vibrational mode. This equation is accurate when the layer attached to the crystal is elastic, i.e., ultrathin and compact. However, when the layer is thick or is infused with solvent, it can have viscous character, which leads to dissipation of vibrational energy and further lowering of the resonant frequency.[20−28] If applied to a viscoelastic layer, the Sauerbrey equation gives an overestimate of the mass actually deposited on the surface. The polymer brush, which is composed of polymer chains that are grafted by one end to the surface, are infused with solvent and are stretched away from the grafting surface toward the bulk solvent, would be expected to be viscoelastic. In the present study, to evaluate the mass of the polymer chains alone, we collapsed the brush into an ultrathin and compact layer to which the Sauerbrey equation could be applied.

## II. Experimental Section

**A. Materials.** The polymer samples used and their characteristics are listed in Table 1. In Table 1, PS means polystyrene and HS-PS means thiol-end-functionalized polystyrene. All polymers were purchased as monodisperse ($M_w/M_n \leq 1.1$) samples from Polymer Source, Inc. (Dorval, Canada). HPLC-grade methanol (>99.9%)

**Table 1. Polymer Samples Used in the Investigation**

| polymer | $M_n$, g/mol | $M_w/M_n$ |
|---|---|---|
| PS-50K | 50 000 | 1.06 |
| HS-PS-5K | 5 300 | 1.10 |
| HS-PS-25K | 25 000 | 1.07 |
| HS-PS-50K | 50 000 | 1.06 |

* Corresponding author. Phone: 215-895-4970. E-mail: lynn.s.penn@drexel.edu.

10.1021/ma8009307 CCC: $40.75 
Published on Web 10/14/2008

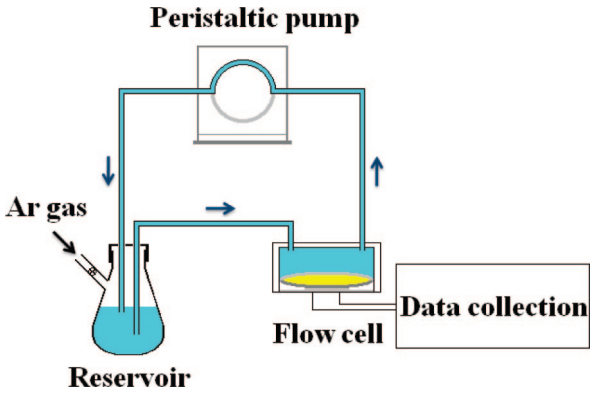


**Figure 1.** The circulating system of QCM for real-time monitoring of formation and behavior of polymer brush on gold-coated crystal inside the flow cell.

and HPLC-grade toluene (>99.9%) were purchased from the Aldrich Chemical Co. The 11-mercapto-1-undecanol (97%) was purchased from Aldrich.

**B. QCM Operation.** An E4 QCM instrument (Q-Sense Inc., Gothenburg, Sweden) was used to monitor the formation of polymer brushes on gold surfaces. In this instrument, the sensing element is an AT-cut piezoelectric quartz crystal disk (14 mm in diameter and 0.3 mm thick) coated with a 100-nm thick layer of gold on one side that acts as the grafting surface and on the other side that acts as an electrode. The crystal vibrates at a resonant frequency of 4.95 MHz ± 50 kHz in the absence of mass deposited from the surroundings. Figure 1 shows a diagram of the QCM system. The crystal resides in a flow cell through which the liquid medium of interest is recirculated, driven by a peristaltic pump. The liquid reservoir is protected by a blanket of argon. The instrument has an inherent sensitivity of 1.77 ng/cm$^2$ (0.1 Hz) of mass deposited.

Prior to use in the QCM, the gold surfaces of the quartz crystals were cleaned with piranha solution to remove impurities. All solvents used in QCM experiments were freshly distilled, degassed, and filtered under argon to remove moisture, $O_2$, and small particles that could stick transiently to the surface of the crystal and cause erratic spikes in the frequency trace. The liquid medium (solution or pure solvent) was pumped by peristaltic pump at a rate of 35 $\mu$L/min through a flow cell containing the gold-coated quartz crystal. The temperature of the system was controlled to 21 °C and liquid media were kept under argon during the experiment.

All experimental solutions of polystyrene in toluene were approximately 1 $\mu$M, which qualifies as dilute. Even though dilute, the solution contained a large excess of solute over the theoretical maximum that would fit on the gold surface. Typically, two replicate experiments were run at the same time in side-by-side flow cells.

**C. Benchmark Experiment.** The process selected as a benchmark was formation of a self-assembled monolayer (SAM) of a hydroxyl-substituted alkanethiol on gold.[29−39] Duplicating the literature procedures[29,30] as closely as possible, we exposed the gold surface of the sensing element of the QCM to a dilute solution (∼1 mM) of 11-mercapto-1-undecanol in ethanol for up to 24 h at room temperature. Our procedure differed from that documented in the literature only in that our gold surface was exposed to a closed, circulating system of degassed solution under argon atmosphere instead of to a static solution in an air atmosphere in a flask.

**D. Test for Segmental Adsorption.** The test for segmental adsorption consisted of continuously monitoring the vibration of the gold-coated crystal for frequency changes while exposing it to a flowing, dilute toluene solution of inert-ended polystyrene (PS-50K; see Table 1) in the QCM.

## III. Results and Discussion

**A. Benchmark Experiment.** Because our experiments on polymer brushes required lengthy, continuous use of the QCM instrument with organic solvent, conditions to which the instrument is rarely if ever subjected, we needed to assess the reproducibility and reliability of the instrument under these conditions. To do this, we duplicated a lengthy process that had been well characterized by other means. The process, formation of a SAM of 11-mercapto-1-undecanol, yields an ultrathin and compact layer to which the Sauerbrey equation can be applied. The QCM technique gave results that agreed well with those reported in the literature, obtained with various other methods. First, the QCM results confirmed the two-stage kinetics of self-assembly,[32,34] i.e., rapid formation of a loose SAM accounting for 80−90% of the final mass, followed by a very gradual increase to final value by 16 h. Second, the QCM results of 3.74 ± 0.47 thiols/nm$^2$ for average packing density were consistent with literature values of 4.7 thiols/nm$^2$ obtained with diffraction methods.[40,41] The slightly lower value obtained with QCM than with diffraction is explained by the fact that QCM detects all areas of the monolayer while diffraction detects only the perfectly crystalline areas. The benchmark experiment verified that the QCM technique is reliable and reproducible for lengthy processes in organic solvent, the conditions under which polymer brushes must be studied.

**B. Test for Segmental Adsorption.** Even a small amount of segmental adsorption in a system where grafting is taking place can profoundly affect the kinetics of formation of a polymer brush, changing it from three-regime kinetics to two-regime kinetics.[42,43] This means that knowledge of whether segmental adsorption occurs is essential. The test for segmental adsorption, made with inert-ended polystyrene of 50 000 g/mol in toluene, indicated that polystyrene exhibits a small amount of segmental adsorption to gold. The dissipation registered by the QCM instrument for the equilibrium amount of adsorbed polymer was nearly negligible, indicating that the Sauerbrey equation could be used for estimation of mass deposited (adsorbed). The frequency change observed (1 Hz, well above the instrument sensitivity limit) corresponded to 17.7 ng/cm$^2$, or one polymer chain per 429 nm$^2$ of gold surface, or 0.0025 chains/nm$^2$. Rinsing with pure, flowing toluene removed the adsorbed mass completely, demonstrating that segmental adsorption of polystyrene to gold is reversible in toluene.

Systems that do not exhibit segmental adsorption display three-regime kinetics for the process of brush formation,[44−48] whereas systems that do exhibit segmental adsorption display two-regime kinetics for the process of brush formation,[42,43] similar to the kinetics of simple polymer adsorption. In addition, segmental adsorption has been demonstrated to produce grafting densities that are higher than those achieved for the same polymer in the absence of segmental adsorption.[42,43] The notion that segmental adsorption would increase grafting seems counter-intuitive, but it must be recalled that individual segments in an adsorbed chain are constantly undergoing adsorption and desorption, so that grafting sites are always available to any reactive chain-end that comes within a bond length of the surface. Furthermore, adsorbed chains are virtually certain to become grafted, whereas some fraction of nonadsorbed chains can diffuse away from the surface before they become grafted. The existence of segmental adsorption for polystyrene on gold in toluene led us to expect, for this system, two-regime kinetics and higher grafting densities than we had found for polystyrene brushes in the absence of segmental adsorption.

**C. Formation and Characterization of Polymer Brushes on Gold Surface.** For the formation of polymer brushes on gold, monodisperse, thiol-end-functionalized polystyrenes were used. The thiol functional group was selected because it is well-known to coordinate strongly to gold at room temperature.[31] Results for grafting of HS-PS-50K to gold from dilute toluene solution are shown in Figure 2, which presents both change in frequency

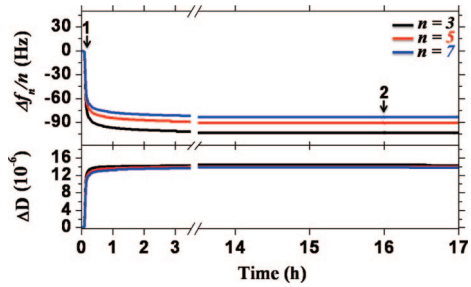


**Figure 2.** Traces of $\Delta f_n/n$ ($n = 3, 5, 7$) and $\Delta D$ vs time for exposure of gold-coated crystal to a solution of thiol-end-functionalized polystyrene (HS-PS-50K) in toluene.

($\Delta f_n/n$) and change in dissipation ($\Delta D$) versus time. When the pure solvent, which established the baseline at 0, was switched to polymer solution (arrow 1 in Figure 2), the frequency dropped immediately, indicating rapid grafting. The figure shows the expected two-regime kinetics, with 90% of the frequency change occurring within the first hour, additional small change occurring slowly over the next few hours, and no further change in frequency after that. The long time without change ensures that the brush has reached saturation, which is the state for which no more chains of the same molecular weight will become grafted to the surface. After it was assured that the brush had reached saturation, the flowing solution was switched back to pure toluene (arrow 2 in Figure 2) to effect rinsing. The brush lost no mass whatsoever upon rinsing, as indicated by the total absence of frequency change. Absence of mass loss provided assurance that all of the polymer chains in the brush were indeed grafted to the gold. If there had been any chains that were not grafted but were merely adsorbed to the gold surface or transiently attached to the brush, these would have been removed by the toluene rinse and a frequency change would have been observed.

In a good solvent, all of the grafted chains of the brush are well-solvated, just as the free chains in a good solvent are well-solvated. When the brush chains and the free chains are chemically identical and are both in good solvent, there is no basis for segment-to-segment attraction between the grafted and free chains. Even so, it is sometimes asked if nongrafted polymer chains are trapped in the brush by means of entanglement with grafted chains. The answer is no, as we showed in a previous study[3] in which a saturated polystyrene brush was exposed to a solution of inert-ended polystyrene chains. The solution was monitored quantitatively as a function of time, and the result was that no free chains were removed from solution for the duration of the experiment. This showed that entanglement of free chains with brush chains *of the same chemical structure* does not occur.[3]

Figure 2 shows two indications that the polymer brush (PS-SH-50K) constructed on the gold surface is viscoelastic rather than purely elastic. The first is a value for $\Delta D$ of $13 \times 10^{-6}$, significantly higher than the designated value of $2.0 \times 10^{-6}$ that separates elastic from viscoelastic layers.[18,19] The second indicator is that the traces for the different vibrational modes, $\Delta f_n/n$ ($n = 3, 5, 7$) are separated rather than superimposed.[18,19] Therefore, the Sauerbrey equation will not give accurate results for this situation. To overcome this inadequacy, we devised a tactic to collapse the brush into an ultrathin, compact layer of sufficient elastic character for valid application of the Sauerbrey equation. This was done by switching the liquid flowing through the flow cell from good solvent to *nonsolvent* for polystyrene. Unfortunately, there is an inherent drawback associated with switching solvent; different solvents exert different electrical and mechanical influences on the vibrating crystal, causing a shift in the baseline. Since we did not want this confounding

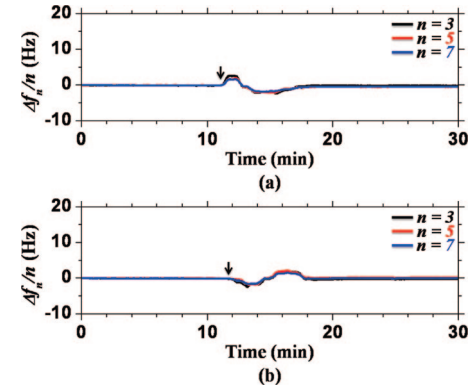


**Figure 3.** Change of solvent on bare, gold-coated vibrating crystal in the QCM. The point of solvent change is indicated by arrow. The baseline re-established itself at the same (zero) frequency for the change in either direction: (a) from toluene to methanol/toluene (4/3) and (b) from methanol/toluene (4/3) to toluene.

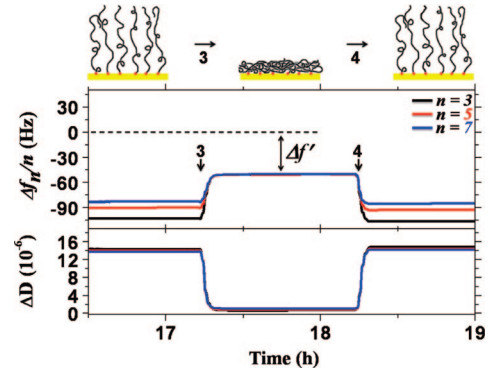


**Figure 4.** Traces of $\Delta f_n/n$ ($n = 3, 5, 7$) and $\Delta D$ vs time for HS-PS-50K, showing collapse and restretching of brush with change of solvent from good to nonsolvent (arrow 3) and 1 h later from nonsolvent to good (arrow 4).

effect on our experiments, we had to find a nonsolvent with the same combined mechanical and electrical influences on the gold-coated vibrating crystal as pure toluene. A trial-and-error approach resulted in identification of a suitable mixed solvent: methanol/toluene in a volume ratio of 4/3. Methanol is a well-known coagulation (precipitation) solvent for polystyrene, and toluene and methanol mixed in the above ratio also produces a coagulation solvent. Figure 3 demonstrates that the switch from pure toluene to mixed solvent does not cause a baseline shift. The same zero baseline originally established by the pure toluene is re-established (after momentary perturbation) by the mixed solvent after the switch is made. The low level perturbation that lasts for about 5−6 min is probably due to diffusional smearing of the front between the pure and mixed solvents as this front traveled over the vibrating crystal in the flow cell. As can be seen from Figure 3, the baseline is the same for either direction of switching, indicating absence of a solvent effect. This means that any frequency change associated with solvent change in the presence of the brush will arise entirely from the change in conformation of the brush itself, as desired.

Figure 4 illustrates the successful use of solvent switching to collapse a brush. The switch to nonsolvent at arrow 3 caused the traces of $\Delta f_n/n$ for $n = 3$, 5, and 7 to be superimposed and the value of $\Delta D$ to fall well below $2.0 \times 10^{-6}$. The superposition of $\Delta f_n/n$ and also the low $\Delta D$ indicate that the brush collapsed into an ultrathin and compact layer, sufficiently elastic for valid application of the Sauerbrey equation.[18,19] When the solvent is changed back to toluene, at arrow 4, the traces of $\Delta f_n/n$ for $n = 3$, 5, and 7 and $\Delta D$ return completely to their nonsuperimposed values, indicating that the collapsed polymer chains have

**Table 2. Masses Deposited and Grafting Density for Polymer Brushes**

| polymer | mass deposited (ng/cm$^2$)[a] | grafting density (chains/nm$^2$) | $R_g$ in toluene[49] (nm) | $R$ in toluene[50] (nm) | $\pi R_g^2/\pi R^2$ |
|---|---|---|---|---|---|
| HS-PS-5K | 549 | 0.623 | 2.4 | 0.72 | 11 |
| HS-PS-25K | 726 | 0.175 | 5.7 | 1.4 | 18 |
| HS-PS-50K | 885 | 0.107 | 8.4 | 1.7 | 24 |

[a] Replicate brush formation experiments, run simultaneously in side-by-side flow cells, differed by less than 5 Hz (<9%) at all points on the time axis. Replicate brush formation experiments run 1 month apart typically differed by 10−13%.

resolvated and stretched away from the surface, into the brush conformation again. We found that the cycle of collapse and restretching could be repeated many times in a completely reversible manner. The transition from brush to collapsed brush is not instantaneous but takes about 5−6 min, coincident with the finite time required for complete replacement of pure solvent by mixed solvent (or vice versa) in the flow cell. Expansion of the time scale in Figure 4 to give a magnified view of the transition revealed no additional information pertinent to the process of conformational change. The mass of the ultrathin, collapsed layer was computed by inserting the frequency difference, indicated by the symbol $\Delta f'$ (Figure 4), into the Sauerbrey equation.

All polymer brushes formed in the present study were collapsed by introduction of nonsolvent, and the masses of the collapsed brushes were determined by means of the Sauerbrey equation. The results are presented in Table 2, in terms of mass/area and grafted chains/area. A common practical criterion for a brush is that $R < R_g$, where $R_g$ is the radius of gyration[49] of a nonstretched chain in good solvent, and $R$ is the lateral dimension of the same chain in the stretched and grafted state.[50] All of the examples in Table 2 substantially exceed this criterion. The last column in the table provides an almost visual way of illustrating that our grafted chains do indeed form a brush. The ratio $\pi R_g^2/\pi R^2$ is equivalent to the number of stretched chains that fit in the lateral area that would be occupied by one hypothetical, nonstretched chain (mushroom conformation). For example, $\pi R_g^2/\pi R^2 = 24$ means that 24 stretched chains are attached to the surface that would be occupied by a single nonstretched chain, or mushroom. The values of $\pi R_g^2/\pi R^2$ in the table correspond to grafting densities at least 50% higher than were achieved in brushes made previously on epoxide-derivatized silicate glass by means of the grafting-to approach.[43] As discussed earlier, the higher grafting density can be attributed to the existence of segmental adsorption during the brush formation process.

**D. Brush Thickness by QCM.** Support that the grafted chains are indeed stretched (i.e., that the layer is a brush) is provided by values of layer thickness calculated with a fitting program that is included in the QCM instrument. In this fitting program, a mathematical description of a viscoelastic layer that has a frequency-dependent response to oscillating strain (vibration) is used in conjuction with the experimental values of $\Delta f_n/n$ and $\Delta D$. The mechanical response of the layer is based on the well-known Voigt element, which is composed of a spring and a dashpot in parallel.[51] The elastic shear modulus, $\mu_1$, of the spring and the viscosity, $\eta_1$, of the dashpot represent the analogous properties of the viscoelastic layer attached to the surface of the vibrating crystal. The unknowns in the computations are $\mu_1$; $\eta_1$; the density, $\rho_1$; and thickness, $d_1$, of layer, which are inserted into the fitting program as initial guesses. Also needed are the density and viscosity ($\rho_2$, $\eta_2$) of the semi-infinite bulk liquid in contact with the viscoelastic layer, both of which can be measured or looked up. Iterations are performed by the program until unique values for $\mu_1$, $\eta_1$, $\rho_1$, and $d_1$ are found

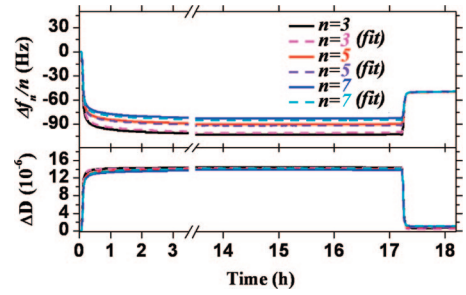


**Figure 5.** Simulated and experimental curves for $\Delta f_n/n$ ($n$ = 3, 5, 7) and $\Delta D$ vs time for HS-PS-50K grafted layer, showing excellent fit for all three vibrational modes.

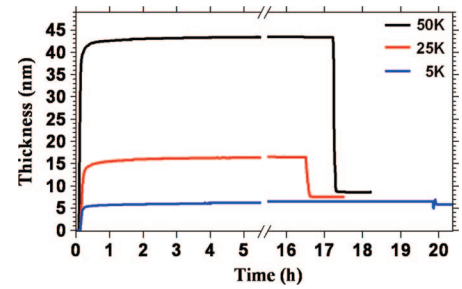


**Figure 6.** Curves of thickness versus time for three polystyrene grafted layers. Solvent switching was used to collapse the HS-PS-50K layer at ~17 h, the HS-PS-25K layer at ~16.5 h, and the HS-PS-5K layer at ~20 h.

**Table 3. Layer Thickness Values for Polystyrene Polymer Brushes**

| polymer | thickness (nm), $d_1$ in good solvent | thickness (nm), $d_1$ in nonsolvent | thickness (nm), $d_1$ from Sauerbrey mass and bulk density[52] [a] |
|---|---|---|---|
| HS-PS-5K | 6.50 | 5.83 | 5.15−5.28 |
| HS-PS-25K | 16.4 | 7.58 | 6.82−6.98 |
| HS-PS-50K | 43.4 | 8.68 | 8.31−8.51 |

[a] Range in values is due to range for polystyrene density (1.04−1.065 g/cm$^3$).

that produce simulated curves that fit the experimental curves of $\Delta f_n/n$ and $\Delta D$. Detailed explanations of how the viscoelastic model relates to $\Delta f_n/n$ and $\Delta D$ are provided in refs 22−24. In our case, experimental data from three vibrational modes, $n$ = 3, 5, and 7, were available for fitting.

Figure 5 compares simulated with experimental curves of $\Delta f_n/n$ and $\Delta D$ versus time for the HS-PS-50K grafted layer. The excellent fit for all three vibrational modes simultaneously indicates that the results of the computations can be viewed with confidence. Similarly excellent fits (not shown) were obtained for simulated curves for grafted layers of HS-PS-25K and HS-PS-5K.

Figure 6 shows values of $d_1$, the layer thicknesses yielded by the fitting program, plotted versus time for all three grafted layers: HS-PS-50K, HS-PS-25K, and HS-PS-5K. The figure shows the rapid buildup of thickness within the first hour of brush formation, the final thickness reached by each brush at saturation, and the immediate reduction in thickness upon exposure to nonsolvent. It is $d_1$ in good solvent, i.e., before collapse, that is the most important feature of a polymer brush, because this value indicates the extent to which the grafted chains are stretched. The before-collapse values (thickness in good solvent), listed in Table 3 for convenience, confirm that these grafted layers are indeed polymer brushes, in which the grafted chains are stretched away from the surface. For all three layers in good solvent, $d_1$ is much greater than $R_g$, the linear dimension characterizing the nonstretched state of a chain in

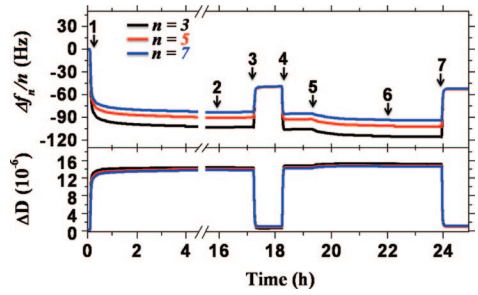


**Figure 7.** Traces of $\Delta f_n/n$ ($n = 3, 5, 7$) and $\Delta D$ vs time for formation of a polymer brush (HS-PS-50K) and subsequent penetration by free chains (HS-PS-5K).

good solvent (see Table 2). The grafted layers of HS-PS-5K, HS-PS-25K, and HS-PS-50K are stretched by factors of 2.7, 2.9, and 5.2 relative to their respective $R_g$ values.

The $d_1$-values for the brush in nonsolvent, i.e., after collapse, are found in the third column of Table 3. It is instructive to compare these thickness values with layer-thickness values calculated independently from Sauerbrey mass divided by the bulk density of pure polystyrene.[52] Results of these calculations are shown in the last column of Table 3. The thickness values in the third column are only about 10% larger than the independently calculated thicknesses in the last column, suggesting that the collapsed layer has excluded most of the solvent.

**E. Penetration Experiments.** Figure 7 shows the full experimental procedure, from formation of a polymer brush $M_n = 50\,000$ g/mol to penetration by free chains of $M_n = 5000$ g/mol. Brush formation started at arrow 1 and continued for some time. The completed brush was rinsed (arrow 2) and was then collapsed (arrow 3) for computation of the mass of grafted chains. Then, the solvent was switched back to good solvent (arrow 4) to restore the brush to its stretched conformation and make it ready for penetration by free chains. At arrow 5, the flowing pure toluene was changed to a dilute toluene solution of free chains, HS-PS-5K. As indicated by the distinct change of $\Delta f_n/n$ to a more negative value (from arrow 5 to arrow 6), these free chains penetrated the brush and added to the mass of the grafted layer. A rinse step with pure toluene (arrow 6) failed to remove any of the mass added, verifying that these small chains were indeed grafted to the gold surface.

This mixed brush, i.e., containing chains of two different molecular weights, was collapsed (right of arrow 7) for evaluation of its mass. The difference in frequency between the collapsed mixed brush and the collapsed original brush represents the mass of the free chains that penetrated the brush and became grafted to the surface. For the system depicted in Figure 7, this difference is relatively small and represents added mass of $43.7 \pm 26.6$ ng/cm$^2$, or $0.0526 \pm 0.0320$ chains/nm$^2$, from three replicate experiments done at different times. (Interestingly, the results for penetration of brushes by free chains showed greater variation than results for formation of brushes, a difference for which there is no obvious explanation.) It is reasonable to suppose that these short chains, surrounded by the long, stretched chains of the original brush, are also in the stretched conformation.

Penetration experiments were conducted similarly for other molecular weight combinations of free chains and brushes, with similar results; only free chains of lower molecular weight than the chains of the brush were able to penetrate. These shorter chains became grafted to the underlying gold surface and could not be rinsed off. A summary of all the experimental results is shown in Table 4, where penetration or no penetration is indicated by yes or no, respectively.

When the free chains in solution had higher molecular weight than the brush chains, $\Delta f_n/n$ ($n = 3, 5, 7$) and $\Delta D$ remained unperturbed, i.e., no changes in frequency or dissipation occurred. This is very significant, because it means that there was not even partial penetration. If free chains had penetrated the brush partially, they would have increased the effective thickness of the brush, thereby lowering the frequency and increasing the viscous character. Both of these would have appeared as changes in $\Delta f_n/n$ and $\Delta D$.

**Table 4. Results for Penetration of Brushes by Free Chains**

| preexisting brush | penetration by free chains: HS-PS-5K | HS-PS-25K | HS-PS-50K |
|---|---|---|---|
| HS-PS-5K | no | no | – |
| HS-PS-25K | yes(70.8 ng/cm$^2$,0.0853 chains/nm$^2$) | no | no |
| HS-PS-50K | yes(43.7 ng/cm$^2$,0.0526 chains/nm$^2$) | yes(35.4 ng/cm$^2$,0.0426 chains/nm$^2$) | no |

These penetration studies show that the polymer brush acts as a selective barrier to free chains. For free chains that are chemically identical to those comprising the brush, the selectivity is based on molecular weight. The underlying physical basis for the selectivity remains a question. Some variables that will be considered in our future work are the size of the free polymer in the coiled conformation (as indicated by $R_g$), the flexibility of the free polymer (as indicated by glass transition temperature of the bulk polymer), and the backbone length of the free polymer (as indicated by contour length). These variables, when considered relative to the same attributes of the chains in the brush, pertain to the ability to diffuse into the brush while coiled, the ability to stretch out to penetrate the brush, and the possible competition between stretched and coiled portions of the free polymer. To make these variables experimentally accessible, we have planned experiments involving well-controlled brushes and free chains that are *not* chemically identical.

## IV. Conclusions

Our study of the penetration of polymer brushes by chemically identical free chains was done on a system composed of thiol-end-functionalized polystyrene chains, toluene, and gold. The study upheld the hypothesis that brushes present a selective barrier to penetration by free chains. Specifically, when brush chains and free chains are chemically identical, only free chains of lower molecular weight than the brush chains penetrate the brush. These chains diffuse all the way to the underlying surface and become grafted, while larger chains do not penetrate even partially.

Our study also showed that the QCM technique works well for continuous and direct monitoring of lengthy processes in organic solvent. To take advantage of the Sauerbrey equation for quantification of the mass of the brush, we applied a solvent change to collapse the brush into an ultrathin and compact layer that excludes most of the solvent. The QCM technique nicely documents the reversible collapse and restretching of the brush.

**Acknowledgment.** This work was supported in part by a grant (CTS0650760) from the National Science Foundation.

## References and Notes

(1) Milner, S. T. *Science* **1991**, *251*, 905–914.
(2) Ionov, L.; Houbenov, N.; Sidorenko, A.; Stamm, M.; Luzinov, I.; Minko, S. *Langmuir* **2004**, *20*, 9916–9919.
(3) Huang, H.; Cammers, A.; Penn, L. S. *Macromolecules* **2006**, *39*, 7064–7070.
(4) Huang, H.; Penn, L. S. *Macromolecules* **2008**, *41*, 2747–2748.
(5) de Gennes, P. G. *Macromolecules* **1980**, *13*, 1069–1075.
(6) Gast, A. P.; Leibler, L. J. *Phys. Chem.* **1985**, *89*, 3947–3949.
(7) Gast, A. P.; Leibler, L. *Macromolecules* **1986**, *19*, 686–691.
(8) Zhulina, E. B.; Borisov, O. V.; Brombacher, L. *Macromolecules* **1991**, *24*, 4679–4690.

(9) Wijmans, C. M.; Zhulina, E. B.; Fleer, G. J. *Macromolecules* **1994**, *27*, 3238–3248.
(10) Aubouy, M.; Raphael, E. *Macromolecules* **1994**, *27*, 5182–5186.
(11) Martin, J. I.; Wang, Z. G. *J. Phys. Chem.* **1995**, *99*, 2833–2844.
(12) Wijmans, C. M.; Factor, B. J. *Macromolecules* **1996**, *29*, 4406–4411.
(13) Pepin, M. P.; Whitmore, M. D. *J. Chem. Phys.* **2001**, *114*, 8181–8195.
(14) Sauerbrey, G. *Z. Phys.* **1959**, *155*, 206–222.
(15) Ward, M. D.; Buttry, D. A. *Science* **1990**, *249*, 1000–1007.
(16) Schneider, T. W.; Buttry, D. A. *J. Am. Chem. Soc.* **1993**, *115*, 12391–12397.
(17) Keller, C. A.; Glasmaster, K.; Zhdanov, V. P.; Kasemo, B. *Phys. Rev. Lett.* **2000**, *84*, 5443–5446.
(18) Vogt, B. D.; Lin, E. K.; Wu, W.; White, C. C. *J. Phys. Chem. B* **2004**, *108*, 12685–12690.
(19) Vogt, B. D.; Soles, C. L.; Lee, H.; Lin, E. K.; Wu, W. *Langmuir* **2004**, *20*, 1453–1458.
(20) Rodahl, M.; Hook, F.; Krozer, A.; Brzezinski, P.; Kasemo, B. *Rev. Sci. Instrum.* **1995**, *66*, 3924–3930.
(21) Caruso, F.; Furlong, D. N.; Kingshott, P. *J. Colloid Interface Sci.* **1997**, *186*, 129–140.
(22) Hook, F.; Rodahl, M.; Brzezinski, P.; Kasemo, B. *Langmuir* **1998**, *14*, 729–734.
(23) Hook, F.; Kasemo, B.; Nylander, T.; Fant, C.; Sott, K.; Elwing, H. *Anal. Chem.* **2001**, *73*, 5796–5804.
(24) Voinova, M. W.; Rodahl, M.; Jonson, M.; Kasemo, B. *Phys. Scr.* **1999**, *59*, 391–396.
(25) Hook, F.; Voros, J.; Rodahl, M.; Kurrat, R.; Boni, P.; Ramsden, J. J.; Textor, M.; Spencer, N. D.; Tengvall, P.; Gold, J.; Kasemo, B. *Colloids Surf. B* **2002**, *24*, 155–170.
(26) Moya, S. E.; Brown, A. A.; Azzaroni, O.; Huck, W. T. S. *Macromol. Rapid Commun.* **2005**, *26*, 1117–1121.
(27) Ma, H.; Textor, M.; Clark, L. R.; Chilkoti, A. *Biointerphases* **2006**, *1*, 35–39.
(28) He, J.; Wu, Y.; Wu, J.; Mao, X.; Fu, L.; Qian, T.; Fang, J.; Xiong, C.; Xie, J.; Ma, H. *Macromolecules* **2007**, *40*, 3090–3096.
(29) Bain, C. D.; Whitesides, G. M. *J. Am. Chem. Soc.* **1988**, *110*, 3665–3666.
(30) Bain, C. D.; Whitesides, G. M. *J. Am. Chem. Soc.* **1988**, *110*, 6560–6561.
(31) Bain, C. D.; Whitesides, G. M. *Science* **1988**, *240*, 62–63.
(32) Bain, C. D.; Evall, J.; Whitesides, G. M. *J. Am. Chem. Soc.* **1989**, *111*, 7155–7164.
(33) Bain, C. D.; Whitesides, G. M. *J. Am. Chem. Soc.* **1989**, *111*, 7164–7175.
(34) Bain, C. D.; Troughton, E. B.; Tao, Y. T.; Evall, J.; Whitesides, G. M.; Nuzzo, R. G. *J. Am. Chem. Soc.* **1989**, *111*, 321–335.
(35) Bain, C. D.; Biebuyck, H. A.; Whitesides, G. M. *Langmuir* **1989**, *5*, 723–727.
(36) Laibinis, P. E.; Fox, M. A.; Folkers, J. P.; Whitesides, G. M. *Langmuir* **1991**, *7*, 3167–3173.
(37) Chidsey, C. E. D.; Loiacono, D. N. *Langmuir* **1990**, *6*, 682–691.
(38) Nuzzo, R. G.; Dubois, L. H.; Allara, D. L. *J. Am. Chem. Soc.* **1990**, *112*, 558–569.
(39) Laibinis, P. E.; Whitesides, G. M. *J. Am. Chem. Soc.* **1992**, *114*, 1990–1995.
(40) Strong, L.; Whitesides, G. M. *Langmuir* **1988**, *4*, 546–558.
(41) Chidsey, C. E. D.; Liu, G. Y.; Rowntree, P.; Scoles, G. *J. Chem. Phys.* **1989**, *91*, 4421–4423.
(42) Huang, H.; Penn, L. S.; Quirk, R. P.; Cheong, T. H. *Macromolecules* **2004**, *37*, 516–523.
(43) Huang, H.; Penn, L. S. *Macromolecules* **2005**, *38*, 4837–4843.
(44) Penn, L. S.; Hunter, T. F.; Lee, Y.; Quirk, R. P. *Macromolecules* **2000**, *33*, 1105–1107.
(45) Penn, L. S.; Huang, H.; Sindkhedkar, M. D.; Rankin, S. E.; Chittenden, K.; Quirk, R. P.; Mathers, R. T.; Lee, Y. *Macromolecules* **2002**, *35*, 7054–7066.
(46) Huang, H.; Penn, L. S.; Quirk, R. P.; Cheong, T. H. *Macromolecules* **2004**, *37*, 5807–5813.
(47) Huang, H.; Fulchiero, E.; Penn, L. S. *J. Polym. Sci., Part A: Polym. Chem.* **2004**, *42*, 5530–5537.
(48) Huang, H.; Rankin, S. E.; Penn, L. S.; Quirk, R. P.; Cheong, T. H. *Langmuir* **2004**, *20*, 5770–5775.
(49) $R_g$ is the radius of gyration in good solvent, computed from $R_g = \alpha\sqrt{C_\infty}/6(n^{1/2}l)$, where $\alpha$ is the expansion factor of a polymer coil in good solvent, $C_\infty$ is the characteristic ratio for polystyrene (equal to 10.8), $n$ is the number of single bonds in the polymer backbone, and $l$ is the length in nm of a single bond.
(50) $R$ is the lateral radius of a circular cross-section of the stretched chain, computed from $[(\text{chains/nm}^2)^{-1} \div \pi]^{1/2}$.
(51) Aklonis, J. J.; Knight, W. J. *Introduction to Polymer Viscoelasticity*, 2nd ed.; John Wiley & Sons: New York, 1983; Chapter 7.
(52) Schrader, D. Physical Constants of Polystyrene. In *Polymer Handbook*, 4th ed.; Brandrup, J., Immergut, E. H., Grulke, E. A., Eds.; John Wiley & Sons: Hoboken, NJ, 1999; pp 91−96.

MA8009307